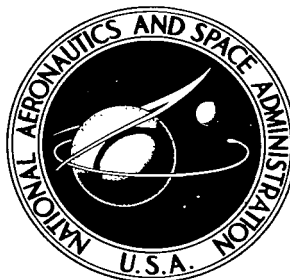


NASA TECHNICAL NOTE



NASA TN D-4054

C/

NASA TN D-4054



LOAN COPY: RETURN TO  
AFWL (WLIL-2)  
KIRTLAND AFB, N MEX

# ACCELERATOR GRID DURABILITY TESTS OF MERCURY ELECTRON-BOMBARDMENT ION THRUSTORS

*by Eugene V. Pawlik and Paul D. Reader*

*Lewis Research Center*

*Cleveland, Ohio*





**ACCELERATOR GRID DURABILITY TESTS OF MERCURY  
ELECTRON-BOMBARDMENT ION THRUSTORS**

**By Eugene V. Pawlik and Paul D. Reader**

**Lewis Research Center  
Cleveland, Ohio**

**NATIONAL AERONAUTICS AND SPACE ADMINISTRATION**

---

For sale by the Clearinghouse for Federal Scientific and Technical Information  
Springfield, Virginia 22151 - CFSTI price \$3.00

# ACCELERATOR GRID DURABILITY TESTS OF MERCURY ELECTRON-BOMBARDMENT ION THRUSTORS

by Eugene V. Pawlik and Paul D. Reader

Lewis Research Center

## SUMMARY

Nine mercury electron-bombardment thrusters were operated for periods of up to 5204 hours. Two thruster sizes were tested that produced 15- and 20-centimeter-diameter beams and were operated at 0.25- and 0.40-ampere ion beam, respectively. The thrusters were operated with 5000 volts total voltage between grids and a net accelerating voltage of 3000 volts in two vacuum facilities. One facility was 5 feet in diameter by 16 feet long and the other was 25 feet in diameter by 70 feet long. The rate of grid erosion was considerably increased in the larger facility where the effects of back-sputtered material were minimized. A maximum accelerator grid erosion rate of 3.6 grams per ampere-hour of accelerator-impingement current was measured. Thruster operation near 80-percent propellant-utilization efficiency exhibited a potential lifetime well in excess of 10 000 hours.

## INTRODUCTION

The mercury electron-bombardment thruster has demonstrated efficiencies and weights adequate for space propulsion mission (refs. 1 and 2). Previous investigations have indicated that, on the basis of short-term tests, the accelerator grid system, operated at reasonable beam density levels, could exhibit lifetimes of the order of 10 000 hours (refs. 3 and 4). Accelerator lifetimes up to 3171 hours have been demonstrated (ref. 5) with small amounts of erosion reported. Backsputtered material from the vacuum-tank walls, however, made accurate erosion predictions for space missions difficult.

The tests described herein were performed to determine whether suitable lifetimes could be obtained when tank backsputtering was reduced to a low level. The program utilized a large vacuum facility to minimize the effects of backsputtered material while

several thrusters were endurance tested. This report analyzes the results of one 20-centimeter-diameter thruster and eight 15-centimeter-diameter thrusters operated continuously over periods ranging from 97 to 4859 hours.

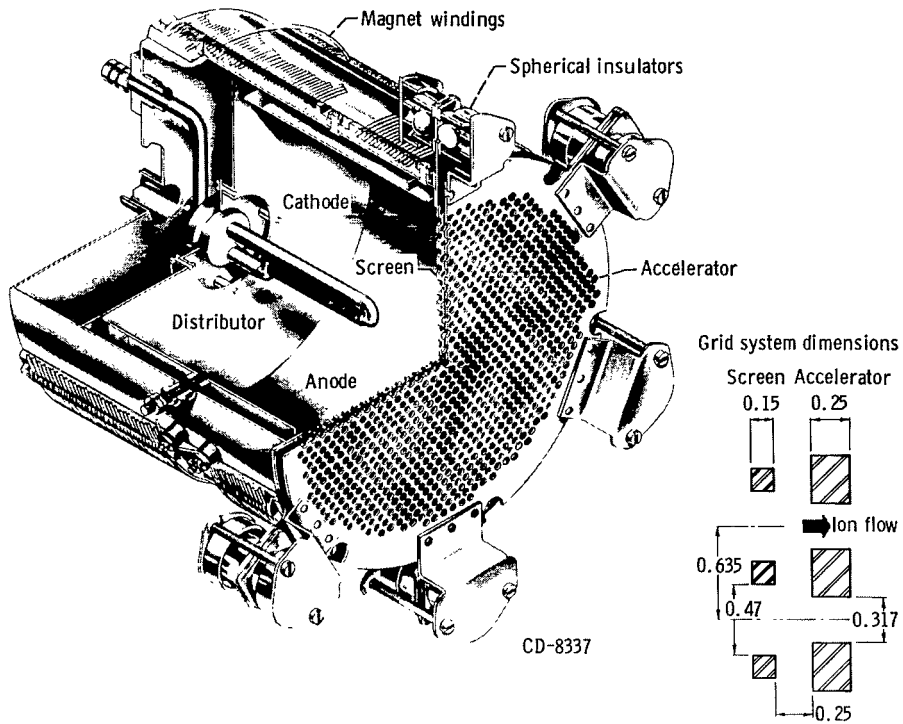
## APPARATUS

### Thruster

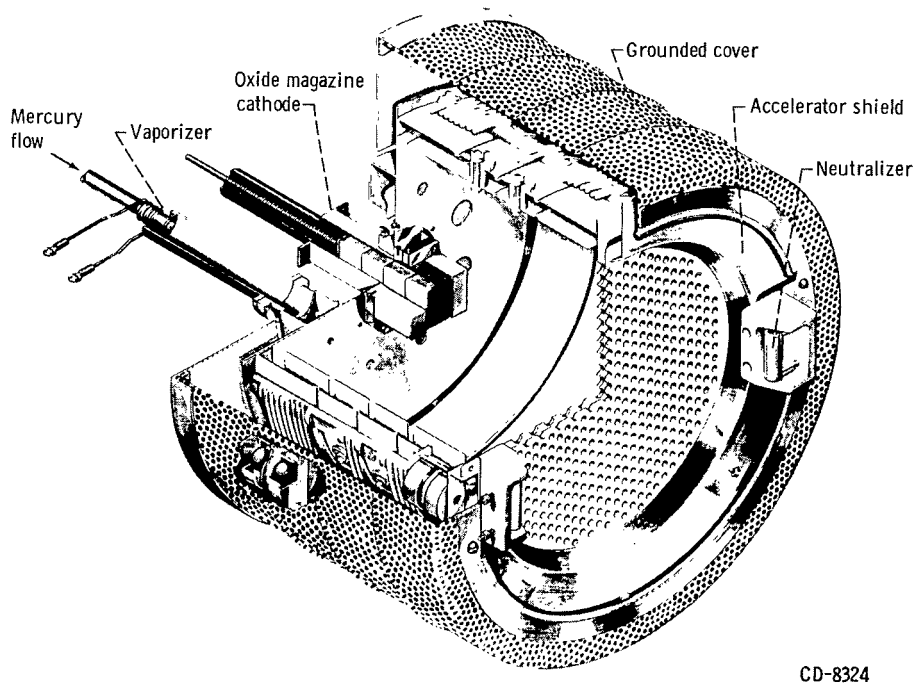
Durability tests were conducted on nine thrusters to evaluate a number of cathode designs simultaneously, since the cathode had proved to be the most critical component. The results of these cathode tests were described in reference 6. Eight of the thrusters were 15 centimeters in diameter, and the ninth was 20 centimeters in diameter. Cutaway drawings of the two thruster sizes are presented in figure 1, and a photograph of a 15-centimeter-diameter thruster is shown in figure 2 (p. 4). Extensive data on the performance of the mercury electron-bombardment thruster is presented in references 7 and 8.

Briefly, the operation of the thruster is as follows: Mercury is vaporized at a heated porous tungsten plug that controls the vapor flow rate and separates the vapor-liquid phase. The mercury vapor passes through the flow distributor into the ion chamber where it is bombarded by electrons emitted from a cathode on the axis of the chamber. A magnetic field surrounding the chamber prevents the electrons from rapidly escaping to the cylindrical anode. Escape to the ends of the chamber is prevented either by operating these ends at the same potential as the cathode or by allowing the thruster body to float and thereby reach an equilibrium with the plasma. Some of the neutral propellant is ionized by the bombarding electrons, and some of these ions reach the perforated screen at the downstream end of the chamber. These ions are accelerated by the potential difference between the screen and the accelerator grids to produce an ion beam. A neutralizer, shown in figure 1(b), then emits electrons to neutralize the ion beam.

The screen and accelerator are drilled molybdenum plates. The thickness, hole sizes, and spacing of the two grids are shown in figure 1(a) and are typical of the grids used on either size thruster. The screen and accelerator grids on thruster 1 differ from this figure inasmuch as modifications were made in order to provide additional information. On one-half of the thruster, the screen holes within a 5-centimeter radius were beveled on the upstream side. On the other half of the accelerator, holes outside of a 5-centimeter radius were enlarged to 0.4 centimeter in diameter. The remainder of the thruster, with the exception of the magnetic field winding, cathode, and insulators, was fabricated of nonmagnetic stainless steel. Small differences in thruster construction existed because modified cathodes, cathode changers, and permanent magnets were used.



(a) 20-Centimeter-diameter thruster. (All grid dimensions are in centimeters.)

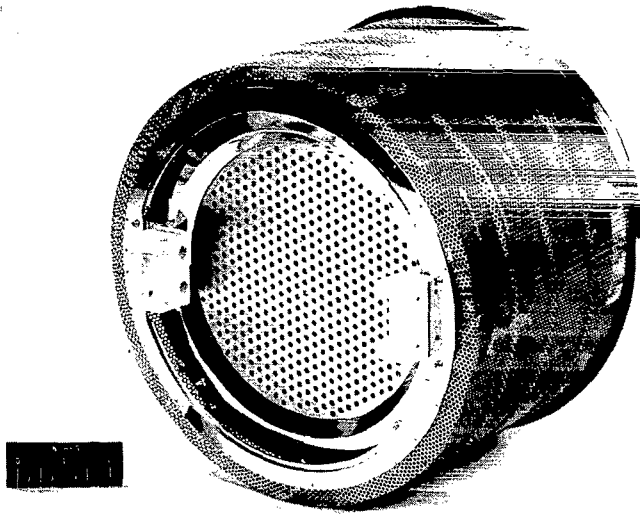


(b) 15-Centimeter-diameter thruster.

Figure 1. - Electron-bombardment.

## Electrical System

A schematic diagram of the electrical system used to endurance test the mercury bombardment thrusters is shown in figure 3. Four control loops were used in these tests but are not shown in the figure. Two control loops were used to keep both the anode and the accelerator voltages constant under varying loads and to recycle these units in the event of a high-voltage arc. A third control loop was incorporated to monitor the accelerator impingement current and to adjust the vaporizer temperature accordingly. The fourth control loop monitored the cathode emission current and utilized the discharge voltage as a control. The control systems are more fully described in reference 5.



C-65-947

Figure 2. -15-Centimeter-diameter thruster.

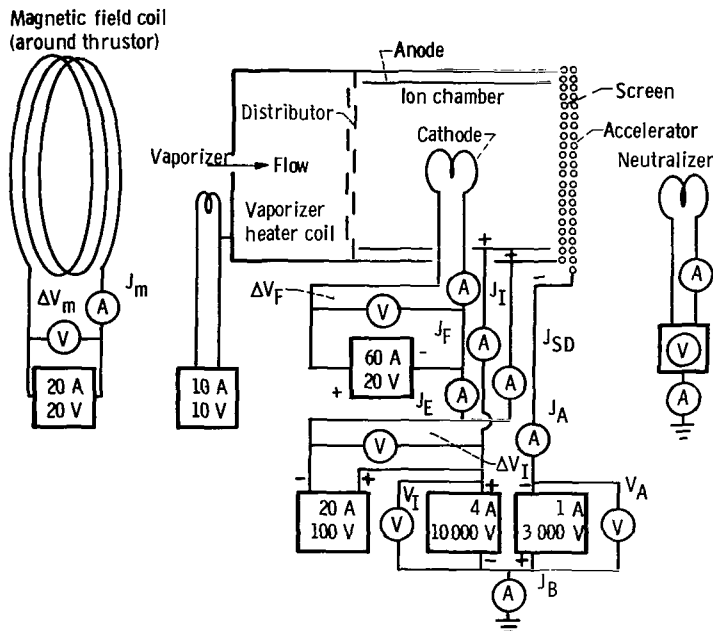
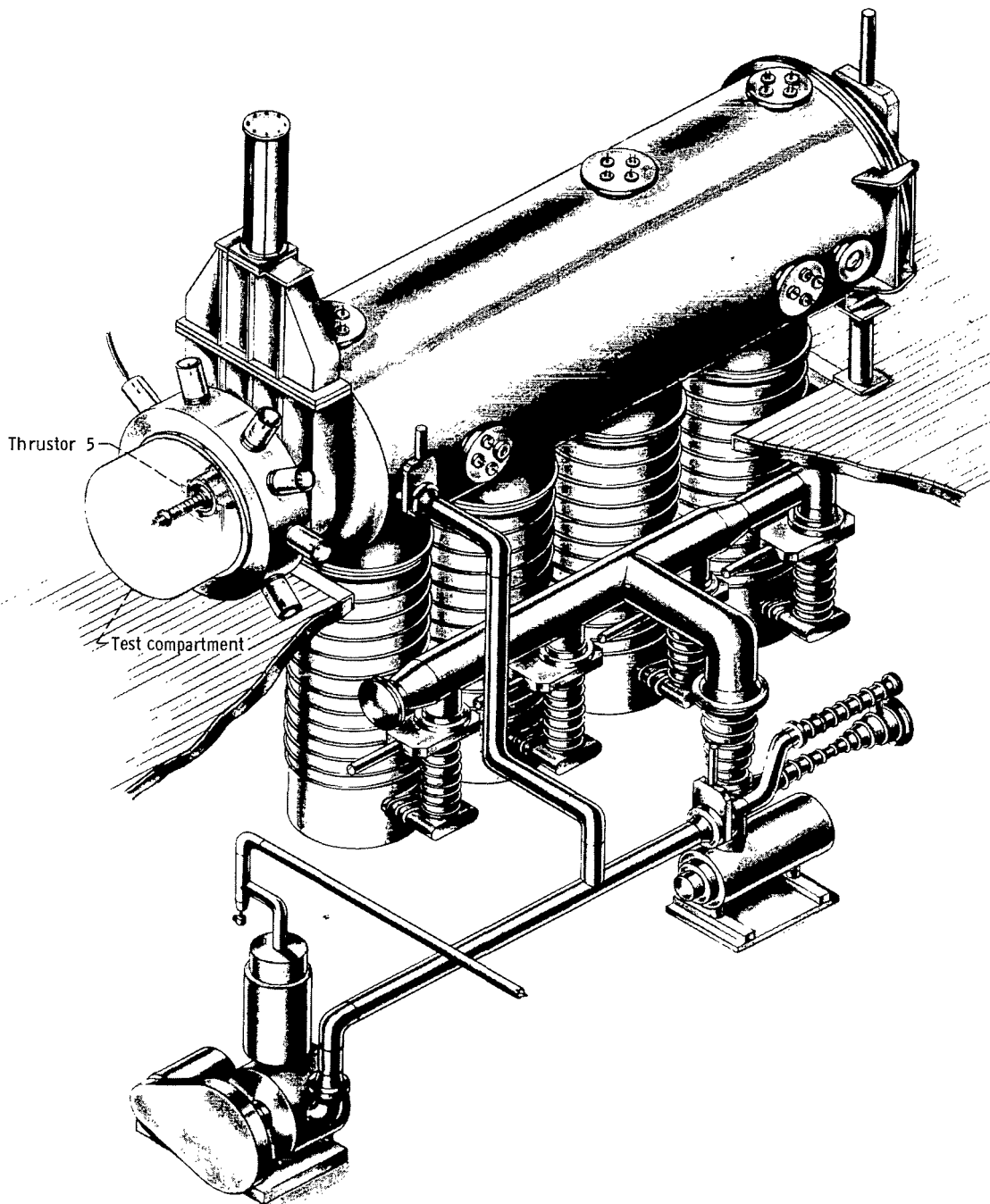


Figure 3. - Schematic diagram of electron-bombardment thruster system.

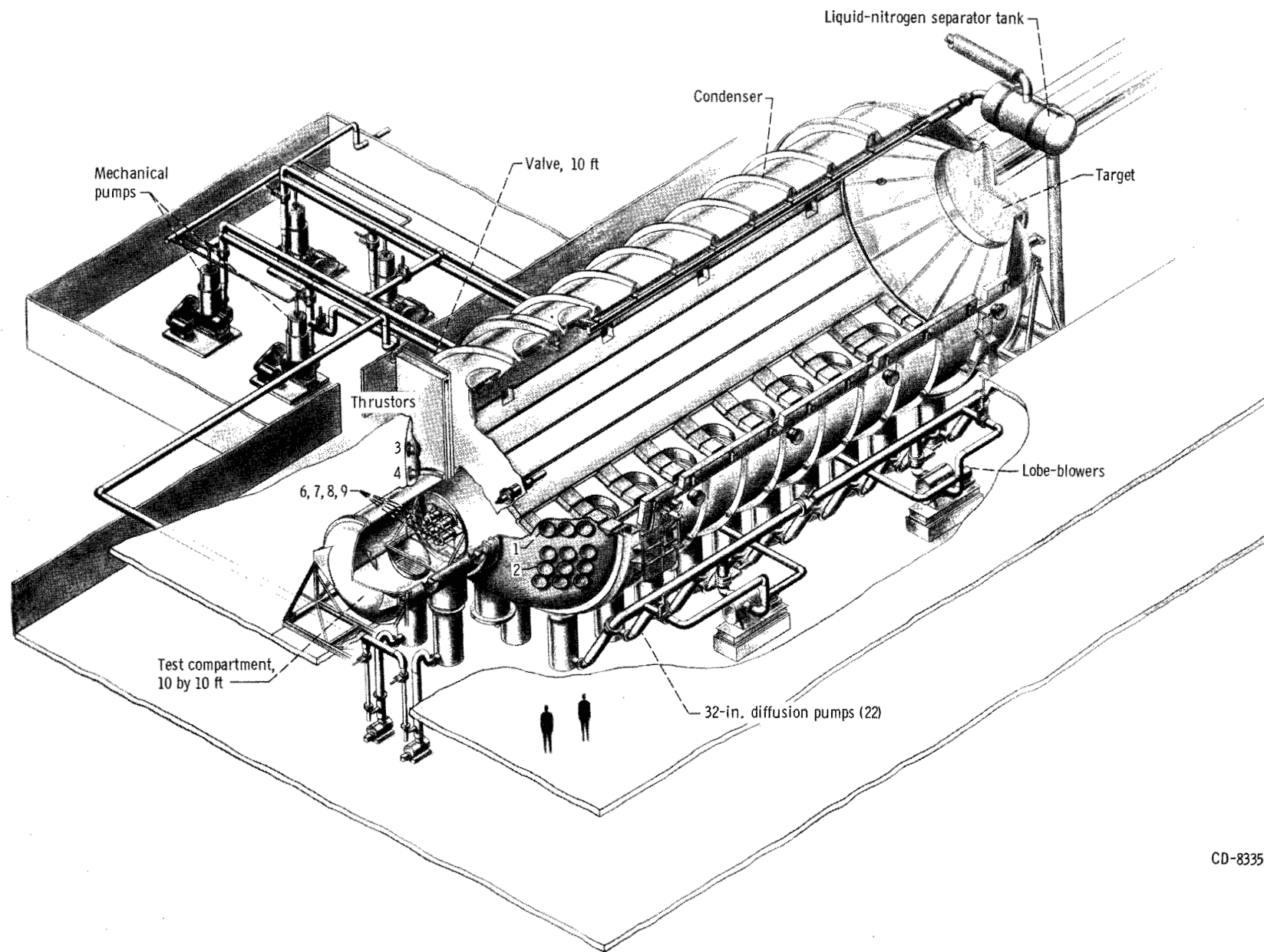
## Facilities

Two vacuum facilities were used to conduct these tests. One thruster (thruster 5) was installed in a 5-foot-diameter, 16-foot-long vacuum tank, as shown in figure 4. This tank has four 32-inch oil diffusion pumps that feed into a common ejector pump then a mechanical pump. Because cryogenic pumping was used in conjunction with these pumps, thruster operation was possible at pressures of



CD-8336

Figure 4. - Thruster installed in 5- by 16-foot vacuum-tank facility.



CD-8335

Figure 5. - Eight thruster stations in 25- by 70-foot vacuum-tank facility.

approximately  $10^{-6}$  millimeter of mercury.

Figure 5 shows the eight thruster stations in the 25-foot-diameter, 70-foot-long vacuum facility (thrusters 1 to 4 and 6 to 9 were located in the 25- by 70-ft facility). The four thrusters (6 to 9) in the 10-foot-diameter, 10-foot-long test compartment could be isolated from the main tank by a 10-foot-diameter gate valve. The tank has twenty-two 32-inch diffusion pumps (two on the test compartment) backed up by four lobe blowers and four rotating piston pumps. With the cryogenic condenser ( $2400 \text{ m}^2$ ) in operation, the facility maintained a pressure of approximately  $10^{-7}$  millimeter of mercury with four thrusters in operation. Only four of the eight thrusters in the facility were operated at one time because of control-system limitations. This tank is described in considerable detail in reference 9.

Both vacuum facilities contained an aluminum honeycomb target that was expected to minimize backspattering. The target was constructed of 0.075-millimeter-thick aluminum. Each honeycomb was 3.8 centimeters long with a length to diameter ratio of 10. Each of the thrusters in the larger facility was aimed at the center of the target.

## PROCEDURE

New grids were installed on each thruster prior to endurance testing. Various endurance tests were then undertaken with these grids. Some preliminary, short endurance tests were made for cathode evaluation purposes. Long endurance tests were then attempted for each thruster, after which various thruster components were evaluated. This report concentrates on the results obtained for the accelerator system. The operating conditions during the endurance tests are presented in table I.

TABLE I. - ELECTRON-BOMBARDMENT THRUSTOR  
OPERATING CONDITIONS FOR DURATION TESTS

Input parameter	Thruster diameter, cm	
	20	15
Anode voltage, V	3000	3000
Accelerating voltage, V	-2000	-2000
Discharge potential, V	18 to 35	18 to 40
Beam current, A	0.400	0.250
Accelerator current, A	0.004 to 0.012	0.002 to 0.010
Emission current, A	3 to 8	3 to 8
Magnetic field, tesla	$15 \times 10^{-4}$	$8.8 \text{ to } 12.9 \times 10^{-4}$
Neutral flow, equivalent, A	0.56 to 0.68	0.29 to 0.57

Prior to each endurance test, the accelerator and screen grids were disassembled and weighed. The grids were then reassembled and the grid spacings were measured in 10 locations. A glass slide was mounted near thrusters 1 to 5 to aid in identifying the amount and species of sputtered material these thrusters received. Weighed amounts of mercury were placed in individual thruster propellant reservoirs located externally to the vacuum facilities. Additional known amounts of mercury were added to these reservoirs as was

necessary during the endurance tests.

After the endurance tests were terminated, the thrusters were removed from the vacuum chamber and the grid spacing was measured again. The mercury remaining in the propellant reservoirs was inventoried, and the accelerator and screen grids were disassembled and their weights recorded. These grids were then cleaned by wire brushing to remove loose backspattered material coating and were reweighed. The erosion data for the screen-accelerator grids are presented in table II.

TABLE II. - EROSION DATA FOR SCREEN-ACCELERATOR GRIDS OF NINE ELECTRON-BOMBARDMENT ION THRUSTORS

Thruster	Grid weight before test		Oper-ating time, hr	Acceler-ator impinge-ment, A-hr	Grid weight after test		Grid weight after cleaning		Total oper-ating time, hr	Average propellant- utilization efficiency, percent
	Screen, g	Acceler-ator, g			Screen, g	Acceler-ator, g	Screen, g	Acceler-ator, g		
1	351.466	482.920	346	1.52	-----	-----	351.490	477.477	----	55
	351.490	477.477	4858	14.08	358.903	432.357	358.345	432.250	5204	63
2	371.579	506.332	281	1.03	371.996	504.921	371.970	504.817	----	69
	371.970	504.817	1809	7.34	375.388	483.499	375.012	483.225	2090	59
3	344.701	508.400	215	0.81	344.933	506.730	344.863	506.691	----	70
	344.863	506.691	2060	6.92	348.221	487.890	348.032	487.847	2275	63
4	365.131	489.769	97	0.39	365.360	488.341	365.344	488.340	----	46
	365.344	488.390	840	2.77	367.461	480.169	367.385	479.938	937	74
5	356.809	514.749	535	2.29	356.491	575.919	355.602	511.285	----	74
	355.602	511.285	141	.59	-----	-----	355.634	508.946	----	--
	355.634	508.946	187	.89	-----	-----	-----	-----	----	--
	-----	-----	4179	11.11	360.710	482.600	356.285	480.380	5042	68
6	369.918	490.357	3224	11.00	378.359	451.616	377.517	451.558	3224	53
7	372.687	488.528	1150	8.42	377.707	463.556	377.392	463.491	1150	44
8	375.041	499.341	158	0.58	370.354	498.315	370.027	498.123	158	45
9	860.466	1419.550	1272	10.48	-----	-----	858.974	1399.220	1272	65

## RESULTS AND DISCUSSION

### Backsputtering

The amount of backsputtering material present on the thrusters tested in the large facility was small. These deposits were removed from several locations. The measured thickness varied to a maximum of 0.02 millimeter for nearly 4000 ampere-hours of total accumulative thruster operation. This thickness was five times lower than that observed for the smaller facility (ref. 5) after 640 ampere-hours of operation. The composition of the backsputtered material was mainly aluminum, copper, and iron, which were sputtered away from the aluminum target, the cryogenically cooled copper baffle, and the stainless-steel tank wall.

An analysis presented in appendix A estimates the amount of sputtered material that might be expected to collect on the thruster for the two tank sizes in this study. The effect of the honeycomb target was not included. For the simple model presented in appendix A, sputtered material would be expected to collect at a rate 30 times greater in the small facility than in the large. The calculated thickness of the collected material after 4000 ampere-hours of operation in the large vacuum tank would be about  $4 \times 10^{-4}$  centimeter. This thickness is about five times less than the observed material deposits. One possible reason for this difference is that the erosion of the neutralizers and their mounts could have contributed to the collected sputtered material.

### Screen Grid Erosion

Examination of the thrusters at the end of the tests indicated that the screen to accelerator grid spacing was close to that originally measured at the beginning of the tests. No severe warping of the grid system was noted indicating that the molybdenum grid system had sufficient dimensional stability over sustained operating periods at elevated temperatures.

Weighings of the screen grids indicated that a grid may either lose or gain weight during an endurance test. The net weight change was the result of two simultaneous processes: material could be removed by ion bombardment from the ion chamber plasma that was maintained at 18 to 40 volts higher than the screen potential; and material could be added by backsputtering from the vacuum tank, the accelerator grid, and the ion chamber. The upstream surface of the screen grid was lightly eroded in each case as a result of ion bombardment from the ion-chamber plasma. This screen erosion existed to the same extent for thrusters that were electrically floating or were at cathode potential. The downstream side of the screen grid was lightly coated with backsputtered material

that adhered quite strongly in most cases. This material was not removed by wire brushing to any extent as shown by a comparison of screen weights before and after they were cleaned. The amount of material added to the screen grid was considerable in some cases. Spectrographic analysis indicated that a large portion of this material was sputtered from the accelerator grid. The change in weight did not represent any serious eroding or dimensional change in the screen-grid geometry.

## Propellant-Utilization Control

The propellant-utilization efficiency, presented for each test in table II, was lower than desired because of the procedure used during the endurance tests. Initial operation of the thrusters indicated that, at accelerator impingement currents of about 1 percent of the ion beam current, a propellant-utilization efficiency of 80 percent or higher was obtained. Therefore, impingement controllers were set to force accelerator currents of 1.0 to 1.5 percent of the ion beam current during the endurance tests. Erosion of the accelerator grids with time, however, decreased the amount of direct impingement. The control loop thus increased the propellant flow until enough charge-exchange ion impingement resulted to raise the total impingement back to the set point. Since the thruster was operated at a constant beam current, a lower propellant utilization resulted. The transmission coefficients for the porous plugs of the vaporizers were checked before and after the endurance tests and were essentially unchanged. The average propellant-utilization efficiency of 63 percent presented for thruster 3 thereby varied from 80 percent at the beginning of the test to 52 percent near the end, as determined from the vaporizer temperatures.

The difficulty in maintaining the desired propellant utilization during the endurance tests indicated that a change or modification of the flow-control procedures is desirable. Any one of the following approaches could be used: (1) incorporate vaporizer temperature instead of accelerator current in the flow-control loop, (2) design accelerator grids to minimize direct ion impingement change with grid wear, (3) utilize another propellant-sensitive output parameter such as thruster ion-chamber performance, or (4) sense the rate of change of the accelerator current with emission-current perturbations instead of the direct current level.

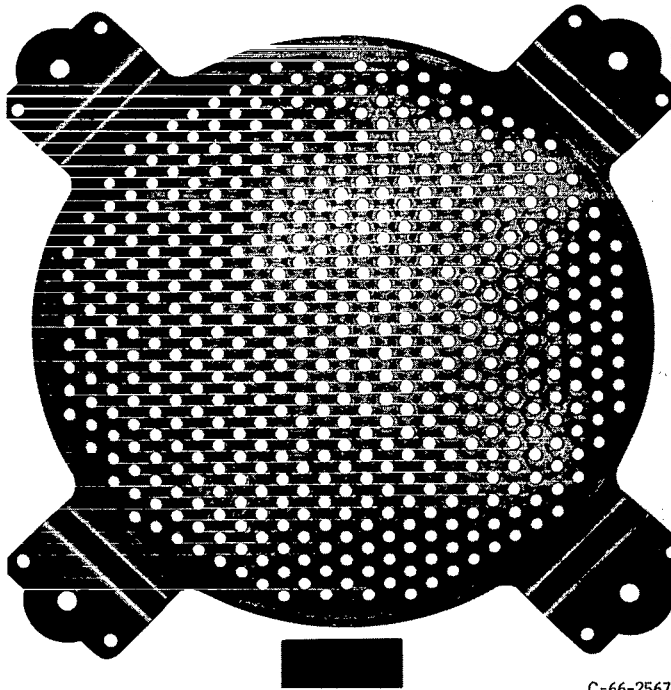
Of these four suggested approaches, utilizing ion-chamber performance seems to be the simplest and the most practical to use because it is a function of discharge voltage, anode current, ion beam current, and propellant utilization. Thruster lifetime considerations indicate that nearly constant values of discharge voltage are desirable. If either ion beam or anode current are maintained constant, the uncontrolled parameter could be used to sense and to adjust the propellant flow. The anode current, for example, when

used in conjunction with a regulated discharge supply and with a constant beam current, is a time-invariant parameter more suitable than is impingement current for propellant flow control. Control sensitivity may vary somewhat with the individual thruster design and might pose a minor problem.

### Accelerator Grid Erosion

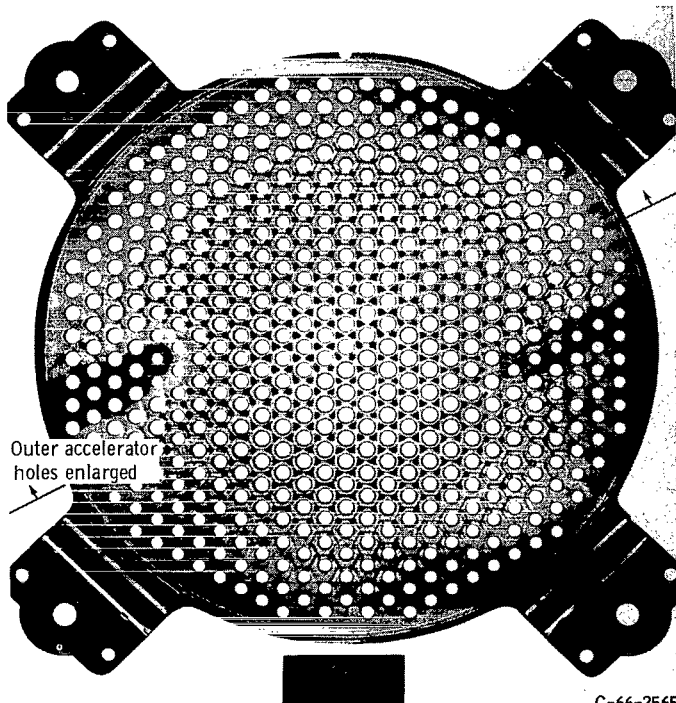
Normal-erosion. - The accelerator grids after operating in excess of 5000 hours are shown in figure 6. The pits between the holes are the usual areas damaged by charge-exchange ions. The depth of these pits varied across the grid diameter. This variation was presumed to be an effect of propellant distribution. The dark regions in figure 6(b) indicate the absence of charge-exchange ions, which is the result of the shielding provided by two immersed neutralizers. The screen holes were blocked in these regions before endurance testing. Because of the blockage, the accelerator holes remained the original size.

Generally, a region of enlarged accelerator holes occurred at the center of the grids. Such enlargement is shown in figure 6(b). However, two accelerator grids (thrusters 5 and 7), presented rather uniform accelerator-hole wear, an example of which is shown in figure 6(a).



C-66-2567

(a) Thrustor 5 after 5042 hours of operation.



C-66-2565

(b) Thrustor 1 after 5204 hours of operation.

Figure 6. - Downstream surface of accelerator grid.

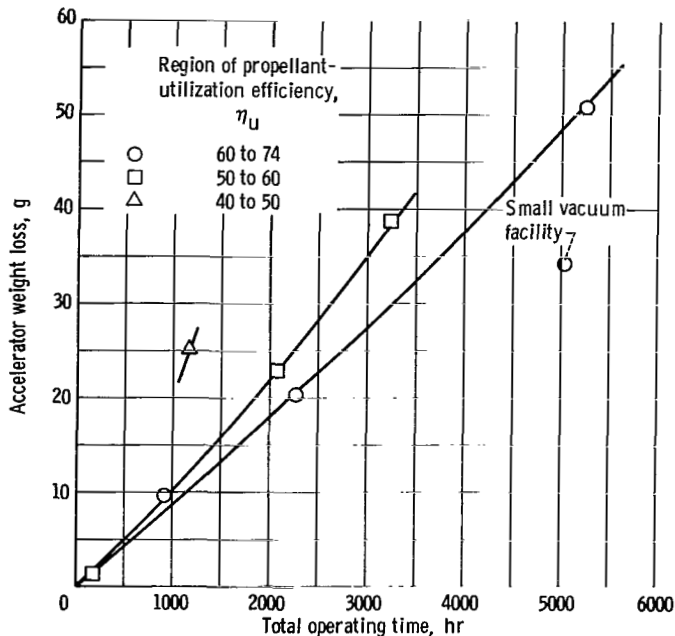


Figure 7. - Accelerator weight loss as function of total thruster operating time for three regions of propellant utilization. Thrustor diameter, 15 centimeters; beam current, 0.250 ampere; anode voltage, 3000 volts; accelerator voltage, -2000 volts.

The accelerator weight loss for the 15-centimeter-diameter thrustor is plotted against total thruster operating time for three regions of propellant-utilization efficiency (fig. 7). The erosion rate, which can be attributed primarily to charge-exchange ions, increased considerably with decreasing propellant-utilization efficiency. The erosion rates for the different regions of propellant-utilization efficiency are in good quantitative agreement with the lifetime calculations of reference 4. The results obtained for the small vacuum tank fell considerably below the rest of the data, which indicated a reduced erosion rate possibly resulting from the high amount of backspattered material.

The accelerator weight loss is plotted as a function of the total accelerator impingement in figure 8. The data obtained for the large vacuum-tank endurance tests again correlate better than the erosion data for the small tank. Excluding the data from the small vacuum tank, the erosion of the accelerator grids varied between 2.7 to 3.6 grams per ampere-hour of impingement.

Sputtering rates of a molybdenum target by mercury ions of various energies are presented for several references in figure 9. The data for the endurance tests of the present investigation are also given. One data point is included from a 150-hour endurance test of reference 10. The sputtering rate of the accelerator grids of the present investigation is much lower than that predicted by reference 11 or 12 for the energy of the ion beam. The exact energy and the angle of incidence, however, are unknown for the ions impinging on the accelerator. The 5000 volts between grids represents a maximum possible value of ion energy if any collection of sputtered material by other parts of the accelerator is ignored, the data of figure 9 indicates that the average impinging ion may have an energy of about 1000 volts or less depending on the angle of incidence. An analog tank study of the accelerator optics (ref. 13) shows that, for similar geometry and current density, the ions fall through a voltage of about one-third of the voltage between the grids and that the angle of incidence can vary from  $0^{\circ}$  to  $90^{\circ}$ . The secondary electron current caused by ion impingement on the accelerator grid has been neglected,

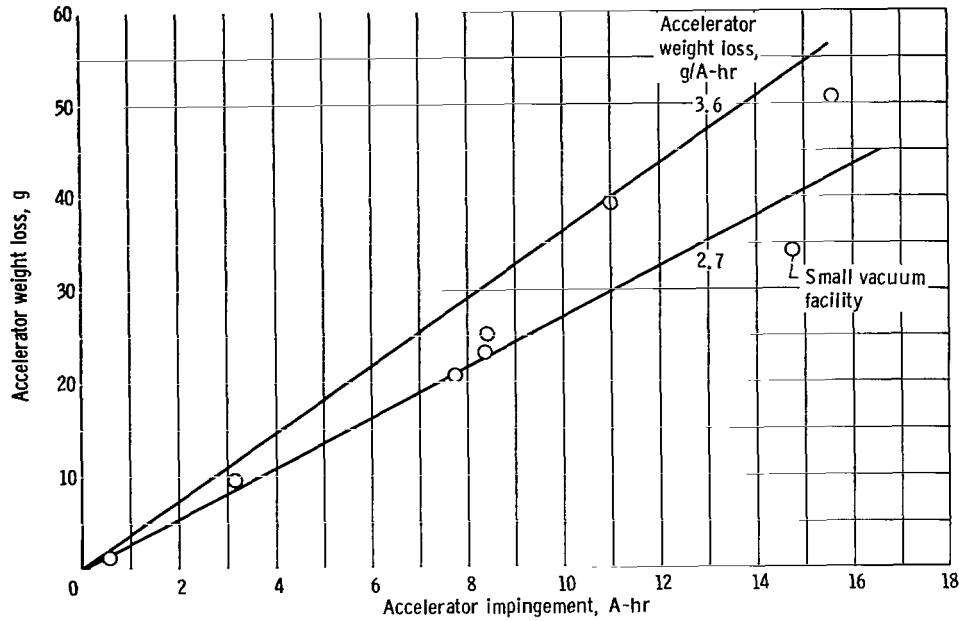


Figure 8. - Accelerator weight loss as function of total accelerator impingement current. Thrustor diameter, 15 centimeters; beam current, 0.250 ampere; anode voltage, 3000 volts; accelerator voltage, -2000 volts.

and the impingement current may therefore be in error by 10 percent or less.

The accelerator holes were measured on both the upstream and downstream grid face. The diameter of the upstream hole was always less than or equal to the diameter of the downstream hole. The ratio of these two hole diameters varied from 1.00 to 1.10 for a hole at the center of the grid and from 1.01 and 1.14 for a hole at the edge of the grid. The hole diameters on the downstream face are presented for several thrusters in figures 10 and 11. Figure 10 shows the observed variations in erosion that ranged from the relatively uniform erosion exhibited by thrusters 5 and 7 to the wide range in erosion exhibited by thruster 6. The amount of erosion of the center hole of thruster 6 was 4.7 times greater than that for a hole at the edge of the grid. The wide variation in erosion rate across the grids is not well understood at this time, but reasons for this variation might exist in the propellant distribution, the accelerator spacing, or the cathode

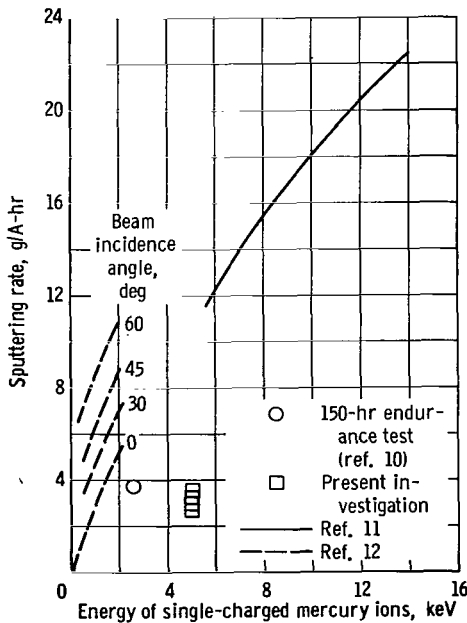


Figure 9. - Sputtering rate of molybdenum target by single-charged mercury ions.

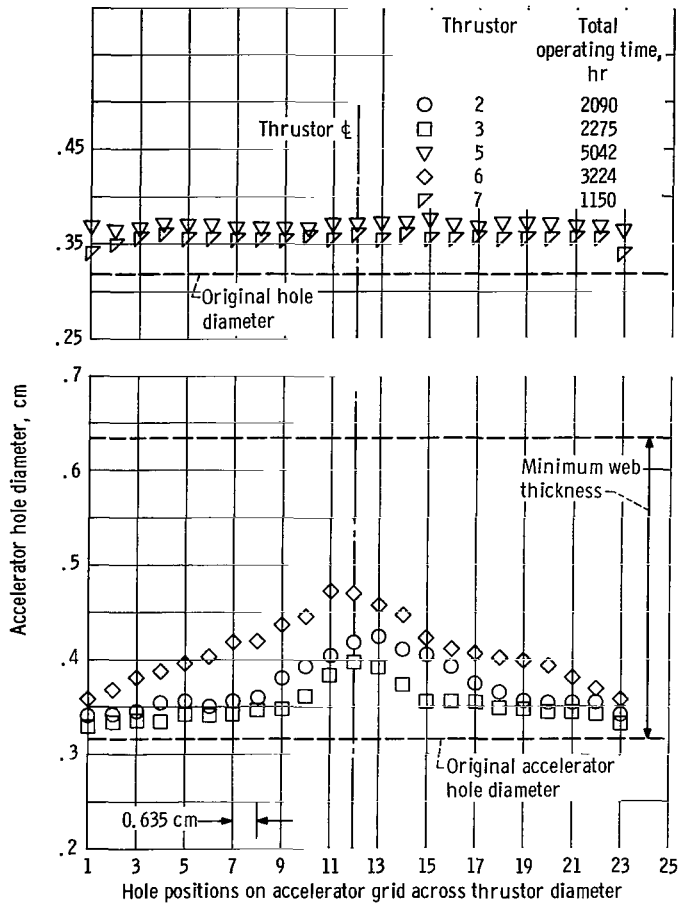


Figure 10. - Diameter of accelerator grid hole across 15-centimeter-diameter thruster after endurance testing. Beam current, 0.250 ampere; anode voltage, 3000 volts; accelerator voltage, -2000 volts.

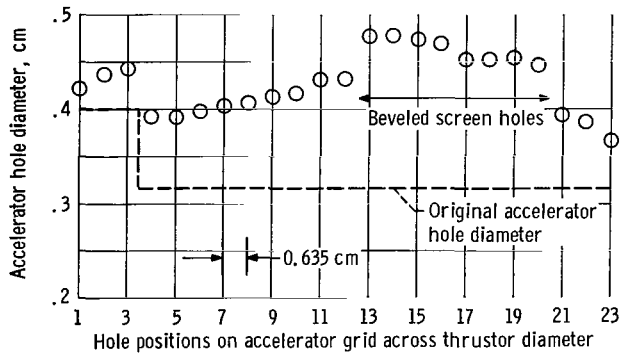
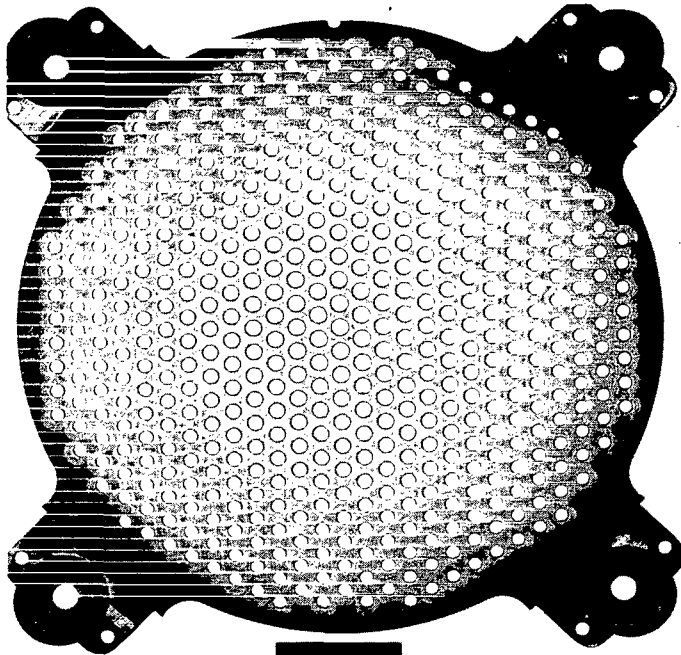
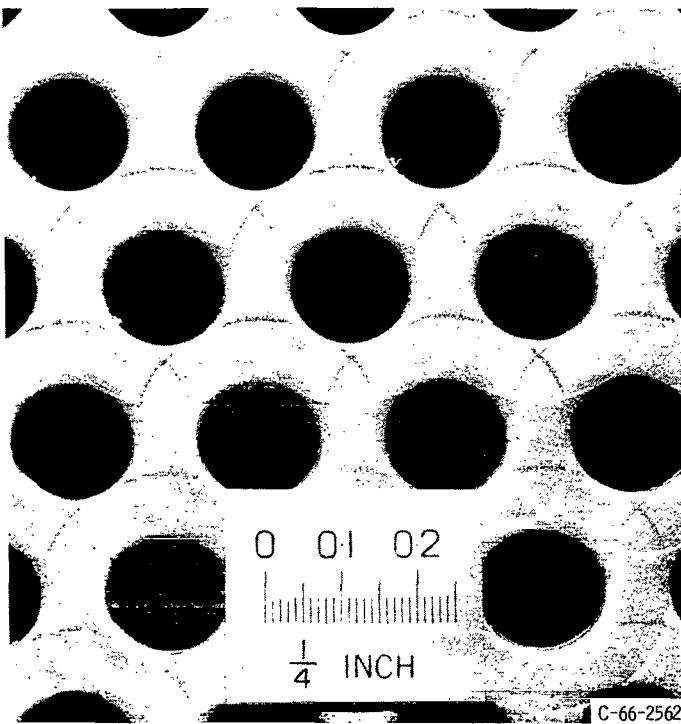


Figure 11. - Diameter of accelerator grid holes across thruster 1 after 5204 hours of operation. Beam current, 0.250 ampere; anode voltage, 3000 volts; accelerator voltage, -2000 volts.



C-66-2564

(a) Upstream surface.



C-66-2562

(b) Center of upstream surface.

Figure 12. - Thruster 6 accelerator grid after 3224 hours of operation.

type or location. Some slight bowing of the grid system existed after manufacturing that could result in a maximum change of 20 percent in the spacing at the center of the grids. Propellant distribution and cathode type varied with the individual thruster, but since no probe measurements were taken in the discharge chamber, the analysis of the aforementioned variables on accelerator grid erosion could only be speculative.

The grids of thruster 1 were modified to include beveled holes in part of the screen; also, some accelerator holes were intentionally enlarged. The accelerator erosion can be seen from the hole measurements presented in figure 11. Beveling the screen grid resulted in an increase in the accelerator erosion rate. The two adjacent holes near the center of the grid, which should be in contact with approximately the same plasma density, showed an erosion rate 35 percent greater on the accelerator hole in line with the beveled screen grid hole. The enlarged accelerator holes exhibited a lesser degree of erosion than did the normal size holes.

Some evidence of direct impingement was noted on the accelerator grids. The upstream surface of the thruster 6 accelerator grid after 3224 hours of operation is shown in figure 12. The grid was lightly coated with sputtered material indicated by the dark area at the

periphery of the grid. Surrounding each screen hole was a circular pattern of direct impingement that had removed the sputtered layer and kept the area of the accelerator grid within the beam diameter. The diameter of the circular pattern around each hole increased slightly from the edge to the center of the grid. The intensity of this direct impingement was greater at the center of the grids where an etched surface could be clearly seen. Figure 12(b) is an enlarged view of this center region. The results for thruster 6 in the center region were indicative of all thrusters where nonuniform grid erosion existed. The same type of pattern shown in figure 12(b) was also observed for thruster 1. Surprisingly, there was no change in pattern between the region of the accelerator system with or without the beveled holds. However, thrusters 5 and 7 had uniform grid erosion, and a change in this pattern was noted. The beam was perhaps better focused into each individual hole, and a smaller area of direct impingement was observed. The upstream surface of the thruster 5 accelerator grid is presented in figure 13.

The rate of grid erosion across the accelerator may be related to the degree of focusing present; therefore, an extremely well-focused beam presents a smaller volume

in the region between grids where charge-exchange collisions might occur. Ions produced in this region close to the center would have a greater probability of passing through without striking the accelerator hole.

The 15-centimeter-diameter accelerator grids used in this study had a total structural weight within the beam diameter of approximately 300 grams. The accelerator lifetime would ultimately be determined by a failure of one of two types: the first type would cause shorting of the grids as a result of loose or electrostatically attracted material; the second type would be an eroding of the accelerator system to the point where large amounts of electron backstreaming would be permitted through large sections of the grid. The structural weight at the end of a grid lifetime would be difficult to predict and would depend on the type of

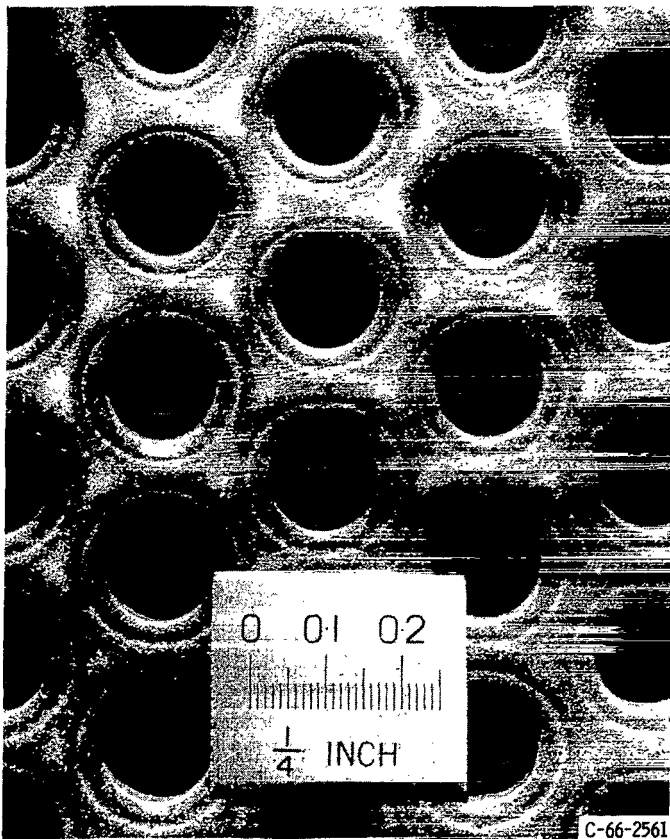
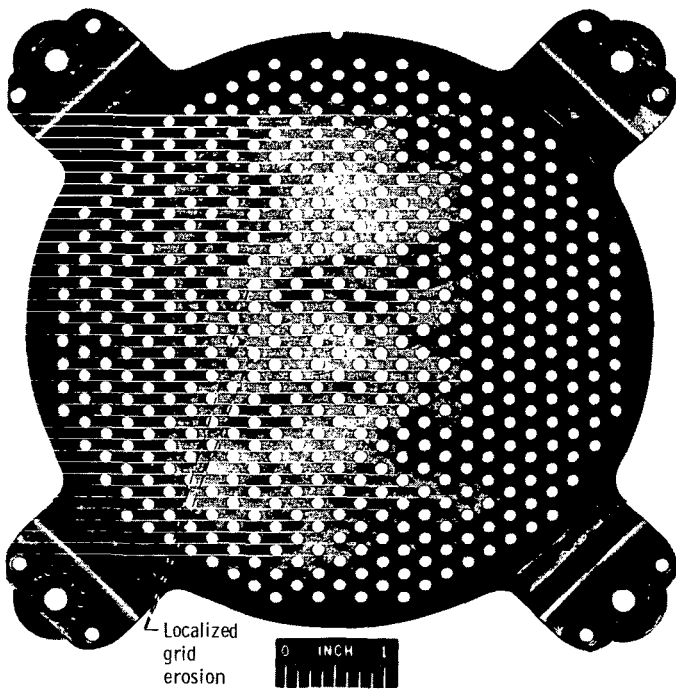
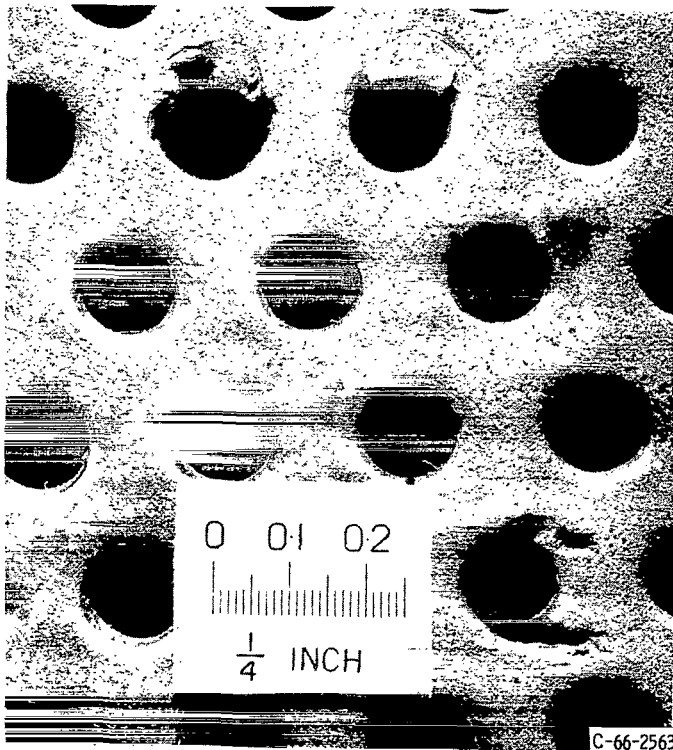


Figure 13. - Center of upstream surface of thruster 5 accelerator grid after 5042 hours of operation.



(a) Downstream surface showing localized grid erosion.



(b) Eroded grid holes on upstream surface.

Figure 14. - Thrustor 8 accelerator grid after 158 hours of operation.

erosion that exists across the grid. It is expected that the grid structure would not fail if the final grid weight within the beam diameter remained in the range of 100 to 200 grams representing concentrated to uniform erosion distribution. The 50.7 grams lost during the 5204 hours that thrustor 1 operated is 16.9 percent of the support structure within the beam diameter and represents 25 to 51 percent of this total allowable erosion, indicating that a lifetime of 10 000 hours could be achieved. The accelerator hole exhibiting the greatest erosion had about 67 percent of the original structure remaining. The impingement conditions for thrustor 1, however, were higher than if the thrustor had been more correctly operated at greater propellant utilization. If relatively uniform erosion could be achieved, a larger amount of mass (possibly 200 g) could be eroded before failure occurred. A reasonable value of impingement current might be 2 milliamperes, which causes erosion at the rate of 3.6 grams per ampere-hour and permits a grid lifetime of 28 000 hours for a 200-gram erosion. Greater lifetimes might be achieved with an increased accelerator grid thickness.

Localized grid erosion. - A rapid erosion of several accelerator grid holes was noted on thrusters 8 and 9. The upstream surface of the accelerator grid from thrustor 8 is shown in figure 14(a). Approximately 2 percent

of the grid holes were worn in an unusual fashion. Figure 14(b) shows an enlarged view of several of these holes. The effects that were observed for thruster 8 existed in an advanced state in thruster 9 where one accelerator grid hole was worn extensively. The downstream surface of thruster 9 is shown in figure 15. The hole was rapidly eroding to the state where electron backstreaming would be permitted.

The reasons for this rapid erosion of certain grid holes are not understood at this time. One explanation is that the erosion may have been caused by burrs on the screen grid. A burr, corresponding to the enlarged hole that was observed, was present on the screen grid of thruster 9. Such burrs could possibly defocus the ion beam and cause greater accelerator grid erosion. However, burrs were not evident in thruster 8, which also exhibited rapid single-hole erosion. Rapid erosion caused by burrs could be eliminated easily by careful inspection during thruster assembly.

### Charge-Exchange Effects

Some unusual effects of charge-exchange ion erosion were observed on the thrusters after endurance testing. An accelerator shield (fig. 1(b), p. 3) located at the outside edge of the accelerator grid was maintained at the same potential as the accelerator. A grounded cover enclosed the thruster and terminated near the accelerator shield. This grounded cover was mounted on a stainless-steel sheet for the test compartment thrus-

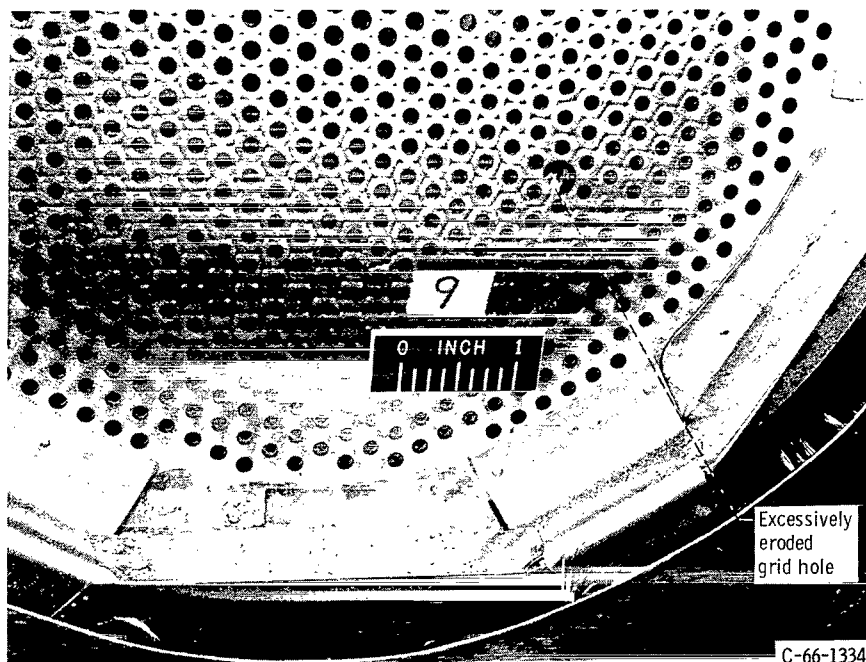


Figure 15. - Downstream surface of thruster 9 after 1272 hours of operation.

tors. During operation, charge-exchange ions were formed within the exhaust plasma and were electrostatically attracted to the accelerator shield, eroding it in a circular pattern as shown in figure 16. The patterns that resulted from this erosion are shown in figures 17(a), (b), and (c) after 1150, 3224, and 5204 hours of operation, respectively. Intense erosion occurred in a circular pattern that was about 20 centimeters in diameter and 0.15 centimeter in width, with interruptions at the neutralizer locations. The neutralizer mounts were constructed of boron nitride and, therefore, could possibly pick up a surface charge and electrostatically repel the ions. The intensity of the erosion varied along the circle and was sufficient to erode completely through the shield in some areas. These areas appear symmetrical and possibly some correlation with the accelerator hole spacing and arrangement might exist.

Several possibilities for the elimination of this problem area are suggested. The grounded covers could be extended to cover more of the accelerator shield, or the accelerator shield could be made thicker. Another approach might be to cover the accelerator shield with a light coating of aluminum oxide that could build a sufficient surface charge to deter this type of erosion.

A second effect of charge-exchange ion erosion was observed in the small vacuum facility. A boron nitride block was used to house a brush-type neutralizer similar to that used in reference 14. A shadow shield was added on the downstream side to minimize

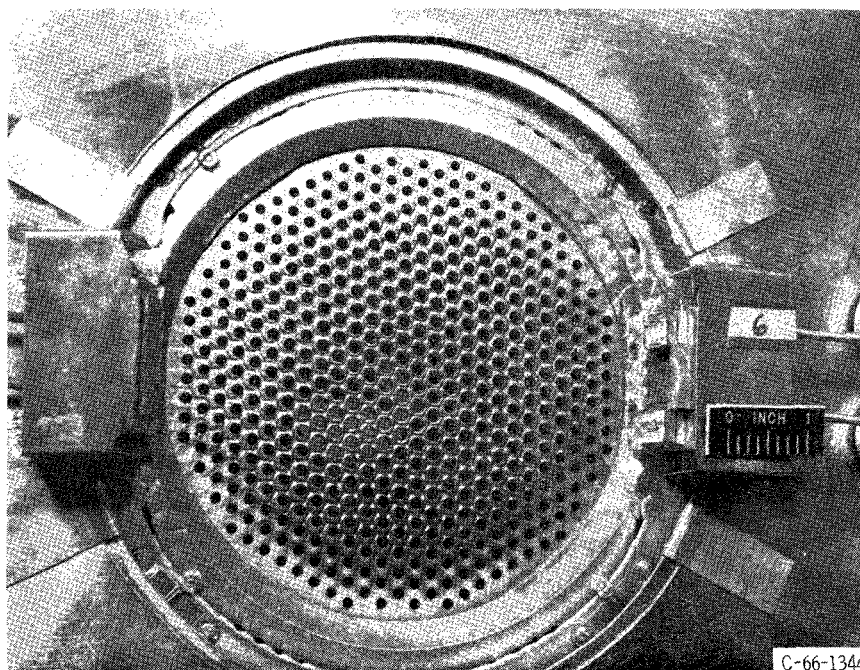
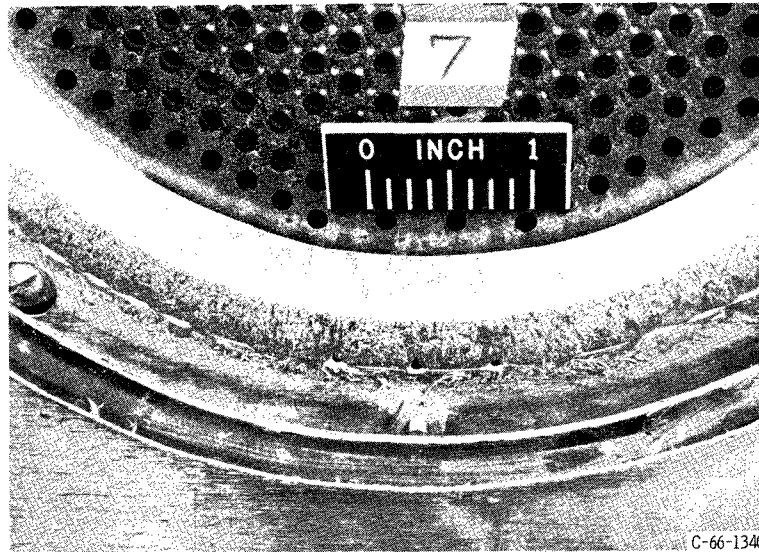
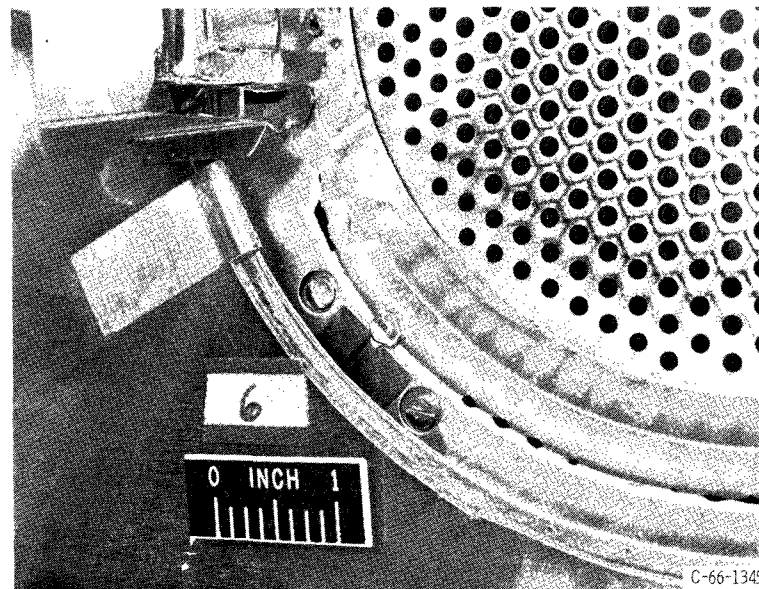


Figure 16. - Accelerator shield of thruster 6 after 3224 hours of operation.



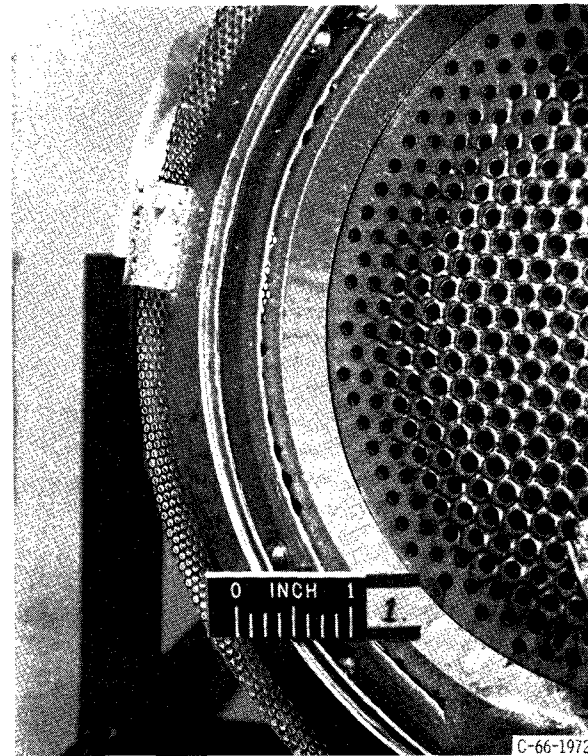
C-66-1340

(a) Thrustor 7 after 1150 hours of operation.



C-66-1345

(b) Thrustor 6 after 3224 hours of operation.



C-66-1972

(c) Thrustor 1 after 5204 hours of operation.

Figure 17. - Charge-exchange erosion on accelerator shield.

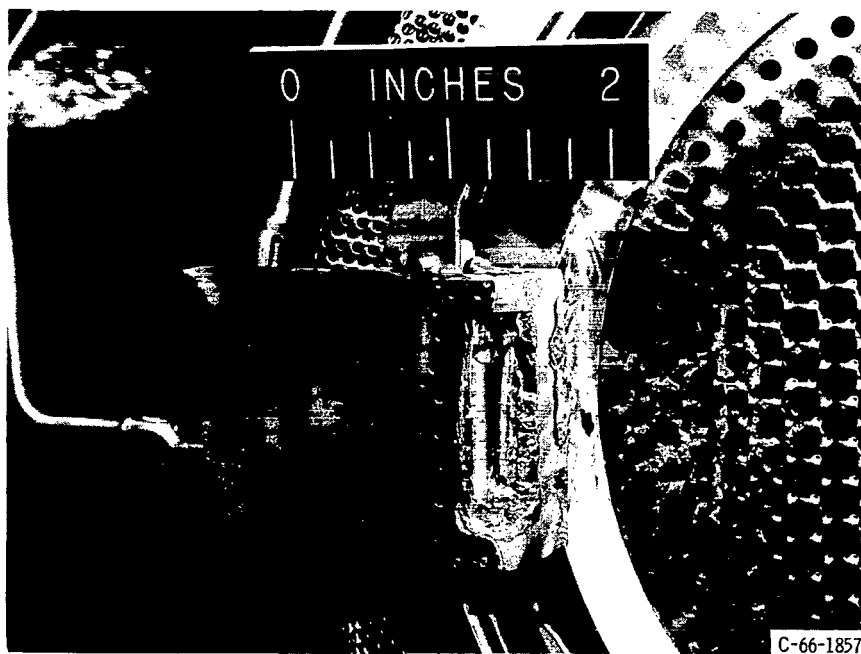


Figure 18. - Charge-exchange erosion on neutralizer shield of thruster 5 after 5042 hours of operation.

coating of the neutralizer by backspattered material. The shield was mounted to a boron nitride block and hence was electrically floating. This shield is shown in figure 18. The edge of the shield near the beam was eroded by direct impingement. A charge-exchange ion erosion was noted on the edge farthest from the beam. This erosion gradually reduced the thickness of the material and wore it completely away at the outermost edge.

## SUMMARY OF RESULTS

The following accelerator system results were obtained from the endurance testing of nine electron-bombardment ion thrusters:

1. Operation of a thruster for 5204 hours resulted in an erosion loss of 16.9 percent of the accelerator grid structure within the beam diameter. This is estimated to represent 25 to 51 percent of the total allowable erosion before possible failure.

2. Accelerator-grid erosion rates were greater in the large vacuum facility where the effects of backspattered material were reduced.

3. Accelerator erosion rates of 2.7 to 3.6 grams per ampere-hour of accelerator impingement current were observed in the large vacuum facility.

4. Variations in accelerator grid erosion across the accelerator diameter were observed. Uniform grid erosion was observed in some tests but the reasons are not well understood at this time.

5. Charge-exchange effects during long-term testing produced considerable erosion of thruster components outside the exhaust beam.

6. Some isolated cases of rapid accelerator grid erosion were observed.

Lewis Research Center,  
National Aeronautics and Space Administration,  
Cleveland, Ohio, November 30, 1966,  
120-23-02-05-22.

## APPENDIX A

### SPUTTERED MATERIAL CALCULATIONS

A mathematical model of the vacuum facilities is presented in order to evaluate the amount of backsputtered material present. A single thruster operating on the axis of the vacuum facility is assumed (fig. 19). If it is also assumed that the ion beam spreads at a fixed angle  $\alpha$  and that the current density decreases in direct proportion to the radial distance from the center of the beam, the expression for the ion beam density  $j_B$  at any point  $(X, r)$  within the vacuum facility is

$$j_B = \frac{3J_B}{\pi \left( \frac{b}{2} + X \tan \alpha \right)^2} \left( 1 - \frac{r}{\frac{b}{2} + X \tan \alpha} \right)$$

where  $J_B$  is the total beam current in amperes. (All symbols are defined in appendix B.) The beam intercepts the wall at the point  $X$  that is expressed as

$$X = \frac{D - b}{2 \tan \alpha}$$

A sticking coefficient of 1 is assumed for all backsputtered material. Material is backsputtered both from the end and the walls of the tank. The amount collected  $S_t$  on the thruster is determined from both sources and is expressed as

$$S_t = S_e + S_w$$

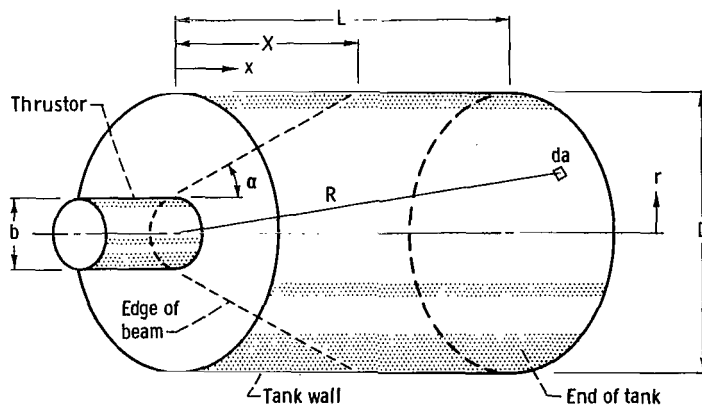


Figure 19. - Schematic drawing of thruster installation in vacuum facility.

where

$S_t$  total sputtered material collected on thruster diameter, g

$S_e$  sputtered material that reaches thruster from end of tank, g

$S_w$  sputtered material that reaches thruster from walls of tank, g

The material sputtered from the tank is assumed to have a cosine distribution and to be independent of the incident angle of the ion. Hence,

$$\frac{d(dS)}{d\Omega} = K j_B t \, da \, \cos \theta$$

where

$K$  sputtering yield, g/A-hr

$t$  time, hr

Since for the cases considered  $R \gg b$ , the solid angle  $\Omega$  (intercepted for each point emitting from  $da$  that will be intercepted by the thruster) will be taken as the projected thruster area divided by  $R^2$ . The material sputtered from the tank end and deposited on the thruster is, therefore, given by

$$S_e = \int -\frac{1}{\pi} K_e j_B t \Omega \cos \theta \, da$$

$$S_e = \int_0^{D/2} \frac{1}{2\pi} K_e j_B t \left( \frac{\pi b^2 \cos \theta}{4R^2} \right) \cos \theta \, 2\pi r \, dr$$

Since  $R^2 \simeq L^2 + r^2$

$$S_e = \frac{3J_B K_e t b^2 L^2}{4 \left( \frac{b}{2} + L \tan \alpha \right)^2} \int_0^{D/2} \left( 1 - \frac{r}{\frac{b}{2} + L \tan \alpha} \right) \frac{r}{(L^2 + r^2)^2} \, dr \quad (1)$$

The back-sputtered material from the walls of the tank is given by

$$S_w = \int \frac{1}{\pi} K_w j_B t \Omega \cos \theta \, da$$

$$S_w = \int_X^L \frac{1}{2\pi} K_w j_B t \left( \frac{\pi b^2 \sin \theta}{4R^2} \right) \cos \theta \pi D dx$$

Since  $R^2 \simeq \left(\frac{D}{2}\right)^2 + x^2$

$$S_w = \frac{3K_w J_B t b^2 D^2}{16} \int_X^L \frac{1}{\left(\frac{b}{2} + x \tan \alpha\right)^2} \left[ 1 - \frac{\frac{D}{2}}{\left(\frac{b}{2} + x \tan \alpha\right)} \right] \frac{x dx}{\left[\left(\frac{D}{2}\right)^2 + x^2\right]^2} \quad (2)$$

Integrating equations (1) and (2) for the case where  $b$  is 1/2 foot (for the 15-cm-diam thruster) and  $\alpha$  is  $15^\circ$  (ref. 12 and neutralizer erosion indicates that the ion beam spreads at about  $15^\circ$ ). For the two vacuum tank sizes to be compared (5-ft diam by 16 ft long and 25-ft diam by 70 ft long), the total material sputtered on the thruster for each tank is given as follows:

Large tank:

$$S_t = (9.04 K_e \times 10^{-6} + 4.58 K_w \times 10^{-6}) J_B t \quad (3)$$

Small tank:

$$S_t = (13.78 K_e \times 10^{-5} + 1.84 K_w \times 10^{-4}) J_B t \quad (4)$$

The thickness of the sputtered material  $T$  is expressed as

$$T \equiv \frac{S_t}{\frac{\pi b^2}{4} \rho} = \frac{4 J_B t}{\pi b^2} \left( \frac{a K_e}{\rho_e} + \frac{c K_w}{\rho_w} \right) \quad (5)$$

where  $a$  and  $c$  are the appropriate geometric factors as determined and presented in equations (3) and (4). For a copper wall and a stainless-steel tank, the thickness of the backsputtered material is

$$K_e \approx 5 \text{ g/A-hr (ref. 10)}$$

$$K_w \approx 20 \text{ g/A-hr (ref. 9)}$$

$$\rho_e = 7.9 \text{ g/cm}^3$$

$$\rho_w = 8.9 \text{ g/cm}^3$$

The total amount collected on a thruster in the large tank is, therefore,

$$S_t = 13.6 J_B t \times 10^{-5}$$

The total amount collected on a thruster in the small tank is

$$S_t = 436.0 J_B t \times 10^{-5}$$

The rate of backspattered material buildup should therefore be about 30 times greater in the smaller vacuum facility. The deposited thickness of the backspattered material in the larger vacuum facility is

$$T = 0.09 J_B t \times 10^{-6}$$

For the case where  $J_B t$  is 4000 ampere-hours, the deposited thickness of backspattered material is

$$T = 3.6 \times 10^{-4} \text{ cm}$$

## APPENDIX B

### SYMBOLS

a, c	approximate geometric factors (determined in eqs. (3) and (4))	t	time, hr
b	diameter of thruster, cm	X	point where ion beam intercepts vacuum wall, m
D	diameter of vacuum tank, m	x	point within vacuum facility, m
$J_B$	total beam current, A	$\alpha$	fixed angle of ion beam spread
$j_B$	ion beam density, A	$\theta$	angle at which sputtered particles leave surface
K	sputtering yield, g/A-hr	$\rho$	density, g/cm <sup>3</sup>
L	length of vacuum tank, m	$\Omega$	solid angle intercepted for each point emitting from da
R	distance from thruster to vacuum tank, m		
r	distance from axis of vacuum tank to point within vacuum facility, m	Subscripts:	
S	backspattered material that reaches thruster, g	e	vacuum tank end
T	thickness of backspattered material deposited, cm	t	total
		w	vacuum tank wall

## REFERENCES

1. Mickelsen, William R. ; and Kaufman, Harold R. : Status of Electrostatic Thrusters for Space Propulsion. NASA TN D-2172, 1964.
2. Reader, Paul D. ; and Mickelsen, William R. : Ion Propulsion Systems for Spacecraft. *J. Spacecraft Rockets*, vol. 2, no. 4, July-Aug. 1965, pp. 577-583.
3. Kerslake, William R. : Accelerator Grid Tests on an Electron-Bombardment Ion Rocket. NASA TN D-1168, 1962.
4. Kerslake, William R. : Charge-Exchange Effects on the Accelerator Impingement of an Electron-Bombardment Ion Rocket. NASA TN D-1657, 1963.
5. Reader, Paul D. : Durability Tests of Mercury Electron-Bombardment Ion Thrusters. Paper No. 66-231, AIAA, Mar. 1966.
6. Reader, Paul D. ; and Pawlik, Eugene V. : Cathode Durability Tests in Mercury Electron-Bombardment Ion Thrusters. NASA TN D-4055, 1967.
7. Pawlik, Eugene V. ; and Nakanishi, Shigeo: Experimental Evaluation of Size Effects on Steady-State Control Properties of Electron-Bombardment Ion Thrustor. NASA TN D-2470, 1964.
8. Reader, Paul D. : Experimental Effects of Propellant-Introduction Mode on Electron-Bombardment Ion Rocket Performance. NASA TN D-2587, 1965.
9. Finke, Robert C. ; Holmes, Arthur D. ; and Keller, Thomas A. : Space Environment Facility for Electric Propulsion Systems Research. NASA TN D-2774, 1965.
10. Reader, Paul D. : Investigation of a 10-Centimeter-Diameter Electron-Bombardment Ion Rocket. NASA TN D-1163, 1962.
11. Magnuson, G. D. : Sputtering Mechanisms Under Ion Propulsion Conditions. Rep. No. AE62-0517, General Dynamics Corp., May 10, 1962.
12. Wehner, G. K. ; and Rosenberg, D. : Mercury Ion Beam Sputtering of Metals at Energies 4-15 kev. *J. Appl. Phys.*, vol. 32, no. 5, May 1961, pp. 887-890.
13. Pawlik, Eugene V. ; Margosian, Paul M. ; and Staggs, John F. : A Technique for Obtaining Plasma-Sheath Configurations and Ion Optics For an Electron-Bombardment Ion Thrustor. NASA TN D-2804, 1965.
14. Kerslake, William R. ; Wasserbauer, Joseph F. ; and Margosian, Paul M. : A Mercury Electron-Bombardment Ion Thrustor Suitable for Spacecraft Station Keeping and Attitude Control. Paper No. 66-247, AIAA, Mar. 1966.

*"The aeronautical and space activities of the United States shall be conducted so as to contribute . . . to the expansion of human knowledge of phenomena in the atmosphere and space. The Administration shall provide for the widest practicable and appropriate dissemination of information concerning its activities and the results thereof."*

—NATIONAL AERONAUTICS AND SPACE ACT OF 1958

## NASA SCIENTIFIC AND TECHNICAL PUBLICATIONS

**TECHNICAL REPORTS:** Scientific and technical information considered important, complete, and a lasting contribution to existing knowledge.

**TECHNICAL NOTES:** Information less broad in scope but nevertheless of importance as a contribution to existing knowledge.

**TECHNICAL MEMORANDUMS:** Information receiving limited distribution because of preliminary data, security classification, or other reasons.

**CONTRACTOR REPORTS:** Scientific and technical information generated under a NASA contract or grant and considered an important contribution to existing knowledge.

**TECHNICAL TRANSLATIONS:** Information published in a foreign language considered to merit NASA distribution in English.

**SPECIAL PUBLICATIONS:** Information derived from or of value to NASA activities. Publications include conference proceedings, monographs, data compilations, handbooks, sourcebooks, and special bibliographies.

**TECHNOLOGY UTILIZATION PUBLICATIONS:** Information on technology used by NASA that may be of particular interest in commercial and other non-aerospace applications. Publications include Tech Briefs, Technology Utilization Reports and Notes, and Technology Surveys.

*Details on the availability of these publications may be obtained from:*

SCIENTIFIC AND TECHNICAL INFORMATION DIVISION  
NATIONAL AERONAUTICS AND SPACE ADMINISTRATION  
Washington, D.C. 20546